Journal of Nuclear Medicine, published on October 30, 2020 as doi:10.2967/jnumed.120.244806

The latest developments in imaging fibroblast activation protein (FAP)

Annette Altmann[1,2], Uwe Haberkorn[1,2,3§], Jens Siveke[4,5]

[1] Department of Nuclear Medicine, University Hospital Heidelberg, Germany

[2] Clinical Cooperation Unit Nuclear Medicine, German Cancer Research Center (DKFZ), Heidelberg, Germany

[3] Translational Lung Research Center Heidelberg (TLRC), German Center for Lung Research (DZL), Heidelberg, Germany

[4] Institute for Developmental Cancer Therapeutics, West German Cancer Center, University Hospital Essen, Essen, Germany

[5] Division of Solid Tumor Translational Oncology, German Cancer Consortium (DKTK, partner site Essen) and German Cancer Research Center, DKFZ, Heidelberg, Germany

Corresponding author:

Uwe Haberkorn, Department of Nuclear Medicine, University Hospital Heidelberg, Im Neuenheimer Feld 400, 69120 Heidelberg

Phone: +49-6221-56-7732; Fax: +49-6221-56-5473; Email: uwe.haberkorn@med.uni-heidelberg.de

Keywords: Fibroblast activating protein, PET, SPECT, imaging, theranostics, FAPI

ABSTRACT

Fibroblast activation protein (FAP), a membrane-anchored peptidase, is highly expressed in cancer-associated fibroblasts (CAFs) in more than 90% of epithelial tumors and contributes to progression and worse prognosis of different cancers. Therefore, FAP is considered a promising target for radionuclide-based approaches for diagnosis and treatment of tumors and for the diagnosis of non-malignant diseases associated with a remodeling of the extracellular matrix. Accordingly, a variety of quinolone-based FAP inhibitors (FAPI) coupled to chelators were developed displaying specific binding to human and murine FAP with a rapid and almost complete internalization. Due to a high tumor uptake and a very low accumulation in normal tissues as well as a rapid clearance from the circulation, a high-contrast is obtained for FAPI-PET/CT imaging even at 10 minutes after tracer administration. Moreover, FAPI-PET/CT provides advantages over FDG-PET/CT in several tumor entities for initial staging and detection of tumor recurrence and metastases including peritonitis carcinomatosa.

Tumor Stroma

Malignant tumors consist of neoplastic cells but also of a variety of non-malignant cells that create and shape the tumor microenvironment, also called tumor stroma. These include cells of the basement membrane and capillaries, immune cells and the heterogeneous population of fibroblast-like cells, termed cancer-associated fibroblasts (Fig. 1). Dysregulated interactions and signaling between the tumor cells and cellular components of the tumor microenvironment representing up to 90% of the tumor tissue in frequently occurring carcinomas of breast, colon and pancreas (*1*) significantly determine the malignant phenotype of cancer cells and contribute to the tumor evolution and progression. Notably, though the production of various growth factors, chemokines and cytokines, non-cancerous stromal cells promote extracellular matrix remodeling, induction of angiogenesis, cellular migration, drug resistance, and evasion of immunosurveillance facilitating invasion and the development of metastasis (*2*).

Cancer-associated Fibroblasts

Cancer-associated fibroblasts (CAFs) account for the majority of the tumor stroma with prominent desmoplastic reactions in colorectal (CRC) (*3*) and pancreatic cancer (PDAC) (*4*) and represent the most prominent modifiers of cancer progression and metastasis. Due to secretion of growth stimulatory, pro-survival and angiogenic factors they promote many different aspects of tumor development including metabolic cooperation, remodeling the extracellular matrix, induction of epithelial to mesenchymal transition and therapy resistance. Moreover, the interaction of CAFs with cellular components of the immune system mediates immunosuppression and inflammation (*5*). CAFs are genetically more stable, and, therefore, less susceptible to the development of therapy resistance than cancer cells per se.

CAFs originate from local fibroblasts, circulating fibroblasts, vascular endothelial cells via endothelial to mesenchymal transition, adipocytes, bone marrow derived stem cells or even from cancer cells via endothelial to mesenchymal transition (*5,6*). This spectrum of origin at least partially explains the phenotypically different subsets of CAFs that promote heterogeneous properties in individual tumor regions (*6*).

Irrespective of origin, the development of CAFs in the tumor stroma is accompanied by morphological and molecular changes leading to spindle-shaped form and the expression of particular surface markers such as the α smooth muscle actin (αSMA), the platelet derived growth factor β (PDGFR β) and the fibroblast activation protein (FAP) (*6*). Whereas many markers are heterogeneously expressed in CAFs in various tumor entities, FAP was shown to be up-regulated in the stroma of more than 90% of epithelial carcinomas (*7*). A recently published meta-analysis involving 15 studies, which assesed FAP expression in 11 solid tumors by immunohistochemistry concluded that FAP was detected in 50 to 100% of the patients and FAP expression is associated with higher local tumor invasion, increased risk of lymph node metastasis and decreased survival (*8*). The association of FAP expression and poor prognosis was most clearly demonstrated in CRC and PDAC, but was also shown for patients suffering from hepatocellular

cancer (HCC) (*9*) and ovarian cancer (*10*). Therefore, FAP is considered as an important target for diagnosis and therapeutic approaches.

Fibroblast Activation Protein

FAP is a type II membrane bound glycoprotein belonging to the dipeptidyl peptidase 4 (DPP4) family with dipeptidyl peptidase and endopeptidase activity and sharing a 52% identity at the protein level with DPP4 (*11*). The protein, which was also given the name seprase, consists of 760 amino acids composed of a short intracellular domain (6 amino acids), a transmembrane domain (20 amino acids) and a large extracellular domain (734 amino acids). Both, the post-proline dipeptidyl peptidase and endopeptidase activity of FAP depend on the catalytic triad consisting of serin (S624), aspartate (D702) and histidine (H734) (*12*) and require homodimerisation of the protein (*13*).

Further to overexpression in CAFs and certain transformed cells of malignant tissues, FAP is also selectively expressed in cells of benign diseases and in normal tissues during remodeling. These include stromal cells and mesenchymal stem cells during embryogenesis, wound healing, fibrotic reactions, and inflammatory conditions such as arthritis, artherosclerotic plaques, fibrosis (*14,15*) as well as in ischemic heart tissue after myocardial infarction (*16,17*). In healthy adult tissues no or only insignificant levels of the protein are detected in uterus, cervix, placenta, breast and skin.

Based on enzymatic or non-enzymatic effects FAP directly enhances proliferation, migration and invasion of stromal fibroblasts and of additional cell types including tumor, endothelial and immune cells leading to invasiveness, extracellular matrix degradation, tumor vascularization, and escape from immunosurveillance (*1,18*). Accordingly, in many human malignancies including CRC, PDAC, ovarian cancer, HCC, and NSCLC, high FAP expression is reported to correlate with a higher local tumor invasion, increased risk of lymph node metastases and decreased survival of patients (*1*).

FAP-specific Targeting of Tumors

The involvement of FAP in tumor development and progression as well as the selective expression of the protein in the microenvironment of the most frequent tumors led to the development of several FAP-based therapeutic approaches. The majority of these strategies focused on the development of inhibitors of the enzymatic activity of the protein and, thereby, the contribution to growth and invasiveness of the tumor. The characterization of the dipeptide substrate requirements for FAP enabled the synthesis of a variety of different small-molecules inhibiting the specific prolyl peptidase activity of the enzyme. Among these, Talabostat, a boronic acid-based inhibitor (Val-prolineboronic acid, PT-100), the only FAP inhibitor tested in clinical studies so far, was well tolerated in solid tumor patients, but despite promising preclinical results failed to induce tumor response in the majority of malignancies in phase II clinical trials (*19*). A combinatorial treatment of Talabostat with either Docetaxel in NSCLC patients (*20*) or Cisplatin in metastatic malignant melanoma patients (*21*) also failed to show any clinical benefit and even reduced survival rate of these patients. Nevertheless, a variety of FAP-specific small molecules has been recently developed providing the basis for new radiopharmaceuticals (*22,23*).

Based on the conflicting data regarding the contribution of FAP's enzymatic activity to tumor progression several therapeutic strategies focused on the restricted tumor expression of FAP and the elimination of FAP-expressing cells. The unique proline-specific proteolytic activity of FAP was utilized to design FAP-activated prodrugs composed of a peptide containing the FAP cleavage site and a cytotoxin that after systemic administration circulate throughout the body in an inactive form (*24,25*). Upon specific binding to FAP and subsequent proteolytic cleavage of the peptide the cytotoxin is able to cross the cell membrane and to reach its intracellular target in FAP-expressing cells but also FAP-negative cancer cells in close proximity (bystander effect). Although most of these strategies showed promising results in different xenograft models regarding tumor regression and toxic side effects were markedly suppressed in comparison with the original drug, clinical application was limited by toxicity of unprocessed protoxin or partial deposition of the active drug in healthy organs (*9*).

Clinical studies demonstrated the ability of FAP-specific antibodies to accumulate in tumor tissues after intravenous application. The ^{131}I-labeled FAP-specific murine antibody F19 originally employed for the identification of FAP as tumor-associated antigen displayed specific accumulation in tumor tissues of colon carcinoma patients. Thereafter, several humanized versions of F19 antibody were prepared and preclinically evaluated for their diagnostic and therapeutic properties in mouse models. Among these, the ^{131}I-labeled anti-FAP antibody sibrotuzumab was applied for the treatment of patients with metastasized FAP-positive carcinomas including breast cancer, CRC and NSCLC and tumor specific accumulation was observed (*26*). However, ^{131}I-sibrotuzumab revealed slow elimination in the liver, the spleen and other normal organs, which was consistent with a slow blood pool clearance. Although an anti-tumor activity of non-labeled FAP antibodies was soon excluded, their excellent tumor stroma targeting properties were exploited for the design of conjugates with toxins or immunomodulatory cytokines for localized delivery (27). Anti-FAP antibodies and anti-FAP scFv and antibody fragments, respectively, coupled to highly toxic substances significantly improved the anti-tumor activity of the substance alone and stimulated the anti-tumor immune response in mouse tumor models (*9*).

Immune-based therapies targeting FAP also include the application of FAP-derived DNA, protein and dendritic cell vaccines to elicit CD8+ and CD4+-mediated immune response against FAP-expressing cells (*9*) and the development of FAP-specific genetically engineered chimeric antigen receptor (CAR) T cells (*28*). Based on T-cell-mediated release of pro-inflammatory cytokines and FAP-specific cytotoxicity, both therapeutic strategies led to elimination of FAP-positive cells *in vitro* and in different mouse cancer models, and induced delayed tumor growth and prolonged survival of the respective animals. Moreover, the combination of FAP vaccination and chemotherapy improved the anti-tumor response in murine CT26 colon carcinoma and D2F2 breast cancer models (*29*). Nevertheless, the limited therapeutic effect combined with occasionally severe side effects prevented so far the clinical transfer of these strategies.

Small Molecule Inhibitors for Imaging and Therapy

The slow clearance of FAP antibodies leading to a high background signal results in a limited sensitivity for the detection of small lesions. This can be encountered by applying radiolabeled small molecules such as MIP-1232 or other FAP inhibitors (*22,23,30*). Therefore, a variety of quinoline-based (*22*) inhibitors were coupled to chelators with specific binding to human and murine FAP with a rapid and almost complete internalization (*31-33*) (Fig. 2). Due to a high tumor uptake, a very low accumulation in normal tissues, and a rapid clearance from the circulation, a high-contrast is obtained for PET imaging even at 10 minutes after tracer administration (*34,35*) (Fig. 3). Usually radioactivity was seen only in the renal pelvis and the bladder, with no accumulation in the renal parenchyma, which is favorable for a possible therapeutic application. Dose estimates for FAPI-02, FAPI-04 and FAPI-46 were in the range of 1.4-1.8 mSv/100 MBq (*34,36*) and, therefore, comparable to other ^{68}Ga-based tracers such as ^{68}Ga-DOTATOC/DOTATATE or ^{68}Ga-PSMA-11. A first comparison with FDG in six patients with different tumor entities showed that except for thyroid carcinoma FAPI-PET/CT showed a better contrast and a higher tumor uptake than FDG. This may be especially important in patients with peritonitis carcinomatosa (*34*) (Fig. 4)

Recently, several new ligands were developed. Moon et al. (*37*) modified a high affinity inhibitor with squaric acid (SA) containing bifunctional DATA^{5m} and DOTA chelators, which showed high tumor uptake and tissue contrast. Besides, ligands were designed for ^{18}F-labeling enabling large scale production for clinical routine application (*38,39*). Toms et al. (*38*) used an ^{18}F-labeled glycosylated FAP inhibitor (^{18}F-FGlc-FAPI). Compared to FAPI-04 (IC_{50} = 32 nM), the glycoconjugate, FGlc-FAPI (IC_{50} = 167 nM) revealed a lower affinity *in vitro*, a higher plasma protein binding and a significant hepatobiliary excretion, but a higher tumor retention in the U87MG glioma model. Furthermore, ^{18}F-FGlc-FAPI demonstrated high specific uptake in bone structures and joints. Giesel et al. (*39*) reported the use of the NOTA-coupled FAPI-74, which can be labeled with both ^{18}F-AlF (Aluminum-Fluoride) and ^{68}Ga in 10 patients with lung cancer. A high contrast with SUVmax >10 was seen at 1 h p.i.. A dosimetry in these patients revealed an effective dose of 1.4±0.2 mSv/100 MBq for ^{18}F-FAPI-74 and 1.6 mSv/100 MBq for ^{68}Ga-FAPI-74, which is lower than the dose obtained with ^{18}F-FDG and other ^{18}F-tracers.

Furthermore, new FAPI derivatives were designed for the labeling with ^{99m}Tc and ^{188}Re, which are available from generators and can be used as a couple for diagnosis and FAP-targeted endoradiotherapy (*40*). The resulting ^{99m}Tc-labeled FAPI tracers showed excellent affinity (IC_{50} = 6.4 nM to 12.7 nM) and binding properties *in vitro* and significant tumor uptake (up to 5.4% ID/g) in biodistribution studies. The lead candidate ^{99m}Tc-FAPI-34 was used for scintigraphy and SPECT in two patients with metastasized ovarian and pancreatic cancer, respectively, for follow-up of ^{90}Y-FAPI-46 therapy (*40*). A comparison to PET/CT imaging with ^{68}Ga-FAPI-46 revealed that ^{99m}Tc-FAPI-34 accumulated in the same tumor lesions with excellent image quality.

Kratochwil et al. (*35*) evaluated FAPI-02 and FAPI-04 uptake in 80 patients with 28 different tumor entities with 54 primary tumors and 229 metastases and discriminated three different groups: the highest average SUVmax (>12) was found in sarcoma, esophageal, breast, cholangiocarcinoma and lung cancer,

an intermediate SUVmax (SUV 6-12) was seen in patients with hepatocellular, colorectal, head-neck, ovarian, pancreatic and prostate cancer and the lowest uptake (average SUVmax <6) was observed in pheochromocytoma, renal cell, differentiated thyroid, adenoid-cystic and gastric cancer. Nevertheless, high variations in uptake were observed across and within all tumor entities.

In 75 patients with 12 different tumor entities Chen et al. (*41*) compared ^{68}Ga-DOTA-FAPI-04-PET/CT with ^{18}F-FDG-PET/CT with respect to their performance in the initial staging (51 patients) and for the detection of tumor recurrence (21 patients). Due to its higher contrast FAPI-04-PET/CT showed a higher detection rate in all 12 types of malignant tumors than FDG-PET/CT (98.2% vs. 82.1%, P = 0.021). The sensitivity of FAPI-PET/CT was also higher in lymph node metastases (86.4% vs. 45.5%, P = 0.004) as well as in bone and visceral metastases such as liver metastases, peritoneal carcinomatosis and brain lesions (83.8% vs. 59.5%, P = 0.004).

The same group evaluated the value of FAPI-PET/CT in 68 patients with inconclusive FDG-PET/CT for the discrimination of mass lesions seen in morphological imaging (n =18), for the detection of unknown primary (n = 6), for staging (n = 21) and for suspicion for recurrence (n = 23). Imaging was followed by a histological analysis as gold standard. Most of the tumor lesions had a higher uptake for FAPI than for FDG and a higher image contrast. This led to a better tumor detection in suspicious mass lesions, in unknown primaries, an upgrade in tumor stage and in disease recurrence with an accuracy of 66.7%, 66.7%, 33.3%, and 87.0%, respectively (*42*).

Furthermore, Shi et al. assessed the value of FAPI-04-PET/CT in 17 patients with suspected hepatic nodules prior to surgery or biopsy and found high uptake in tumor nodules as opposed to one benign nodule (*43*).

In patients with brain tumors (five IDH-mutant gliomas, 13 IDH-wildtype glioblastomas) IDH-wildtype glioblastomas and grade III/IV gliomas, but not grade II IDH-mutant gliomas showed elevated tracer uptake. In glioblastomas, spots were found with increased uptake in projection on MRI contrast-enhancing areas. Immunohistochemistry revealed FAP-positive cells with mainly elongated cell bodies and perivascular FAP-positive cells in glioblastomas and an anaplastic IDH-mutant astrocytoma. If these data are confirmed in larger patient numbers, it seems possible that FAPI-PET/CT may allow non-invasive distinction between low-grade IDH-mutant and high-grade gliomas (*44*).

FAPI-PET/CT has also been used for radiation therapy planning in patients with glioblastoma, head and neck tumors and lower gastrointestinal tract tumors (*45-47*). In 13 patients with glioblastoma the target volume delineation with MRI and FAPI-PET/CT showed significant variations resulting in a larger volume when FAPI-PET/CT and MRI were used in combination for treatment planning (*45*).

Since head and neck cancers show a diffuse growth pattern, differentiation between tumor and healthy tissue can be challenging. Therefore, it can be expected that high contrast images such as those obtained by FAPI-PET/CT may improve therapy planning. Syed et al. (*46*) used four different thresholds (three-, five-, seven- and tenfold increase of FAPI tumor-to-normal tissue ratio) for the calculation of four different gross tumor volumes (FAPI-GTV), which were compared to GTVs obtained by CE-CT and MRI. The quantitative analysis revealed a high FAPI tumor uptake (primary tumors SUVmax 14.62 ± 4.44) vs a

low tracer accumulation in healthy tissues such as the salivary glands (SUVmax 1.76 ± 0.31). Concerning radiation planning the GTV obtained with CE-CT and MRI was of 27.3 mL, whereas FAPI derived contours resulted in significantly different GTVs of 67.7 mL (FAPI × 3), 22.1 mL (FAPI × 5), 7.6 mL (FAPI × 7) and 2.3 mL (FAPI × 10). The combination of the morphological methods with FAPI-PET/CT revealed median volumes, that were significantly larger with FAPI × 3 (54.7 mL, + 200.5% relative increase, p = 0.0005) and FAPI × 5 (15.0 mL, + 54.9%, p = 0.0122).

For tumors of the lower gastrointestinal tract (n = 22) a high tumor- to-background ratio of more than three was found in most tumor lesions. In treatment-naïve patients (n = 6) the TNM classification was changed in 50% and in 47% of patients with metastases (n = 15) new lesions were seen. High, medium and low changes of therapy were observed in 19%, 33% and 29% of the patients, respectively. Furthermore, in almost all patients an improved target volume delineation was obtained when using the image information of ^{68}Ga-FAPI-PET/CT (*47*).

For all three tumor entities future prospective studies are needed to assess the impact of FAPI-PET/CT based radiation therapy on tumor recurrence and survival. If positive, the higher contrast between tumor and normal tissues may allow an automatically performed delineation of tumor volume and, thereby, improve the inter-physician variability during therapy planning.

Besides its expression in malignant tumors, FAP expression is up-regulated in a variety of benign diseases such as myocardial infarction, fibrosis of several organs, rheumatoid arthritis, and artherosclerotic plaques (*14-17*); an example of a patient with tumor and fibrosis is shown in Figure 5. For rheumatoid arthritis murine models imaged with PET and SPECT using radiolabeled anti-FAP antibodies demonstrated a high tracer uptake in the inflamed joints and a correlation of tracer accumulation with the severity of the disease (*48-50*).

In general, auto-immune triggered diseases are associated not only with inflammatory reactions but also with an activation of fibroblasts finally resulting in fibrosis and organ damage. In that respect IgG4-related disease (IgG4-RD) is characterized by autoimmune inflammation associated with fibrosis predominantly found in pancreas, biliary tree, salivary glands, the kidney, aorta and other organs. Two studies evaluated the performance of FAPI-PET/CT as compared to FDG-PET/CT in IgG4-RD (*51,52*).

Employing FAPI-PET/CT for examination of 26 patients with IgG4-RD-related 136 lesions Luo et al. (*51*) additionally detected 13% disease associated changes in organs of 50% of these patients. This led to a higher detection rate of disease manifestation in pancreas, bile duct/liver, and lacrimal glands. With regard to the accumulation of both tracers in disease lesions the authors detected a significantly higher FAPI uptake when compared to the FDG uptake, which was attributed to the presence of activated fibroblasts. However, in IgG4-related lymphadenopathy FAPI showed no accumulation, a finding, which was explained by a lack of fibrosis.

Using FAPI- and FDG-PET/CT as well as MRI and histopathological assessment Schmidkonz et al. (*52*) studied 27 patients with inflammatory, fibrotic and overlapping manifestations of IgG4-related disease. Their evaluation revealed that FDG-positive lesions consisted of dense infiltrations of IgG4+ cells in histology, whereas the analysis of FAPI-positive lesions revealed abundant activated FAP-positive

fibroblasts. Therefore, a discrimination between inflammatory and fibrotic activity seems possible. In addition, fibrotic lesions showed a reduced response to anti- inflammatory treatment as compared to inflammatory lesions. The authors see a potential for changes in therapy with individualized treatment strategies depending on the extent of fibrosis or inflammation. In the former case, specific antifibrotic agents may be preferable to anti-inflammatory therapy.

Another area of interest are cardiac diseases. In an experimental setup, Varasteh et al. studied remodeling processes in rats after sham-operation and coronary ligation for the induction of myocardial infarction (*53*). FAPI uptake in the diseased myocardium showed a peak at six days after coronary ligation, mainly localizing at the border zone of the infarction as shown by autoradiography and conventional staining. The FAPI-positive area was FDG-negative but positive in immunofluorescence in myofibroblasts. This may have a significant impact on diagnosis and the determination of prognosis as well as on the clinical management of these patients.

A further possible application is mentioned in a case report of a patient with PDAC undergoing restaging after therapy with gemcitabine in combination with nab-paclitaxel followed by a modified FOLFIRINOX protocol (*54*). Besides FAPI uptake in the primary tumor, multiple liver metastases, and peritoneal carcinomatosis a high tracer accumulation was seen in the left ventricular myocardium. The authors speculate that the detection of myocardial damage after chemotherapy using FAPI-PET/CT may be useful for the detection and early management of cardiotoxicity.

Since the FAPI ligands are chelator-based containing DOTA, these molecules may be also used for therapeutic applications. A first preclinical therapy application of FAPI-04 was performed in nude mice bearing human pancreatic PANC-1 cancer cells (*55*). In this model high FAP expression was shown by small animal PET imaging and immunohistochemistry. Therapy was done by administration of 34 kBq ^{225}Ac-FAPI-04 and resulted in a significant tumor growth delay compared to non-treated controls without a significant change in body weight. Clinically, few data exist for FAPI-04. In a first patient with metastasized breast cancer in final stage, FAPI-04 with ^{90}Y (half-life 64 hrs) was chosen to match the physical half-life of the therapeutic radionuclide to the tumor retention time. After administration of a relatively low dose of 2.9 GBq ^{90}Y-FAPI-04, the visualization of the metastases in Bremsstrahlung images was possible even at 24 hrs p.i. (*33*). Clinically, no therapy related side effects and especially no hematotoxicity was observed, while a significant reduction in opioid dosing given as pain medication was reported.

Since in tumors the origin, number and distribution of FAP-expressing CAFs as well as the number of FAP molecules per cell may differ, we may expect varying tumor uptake as well as variations in the intratumoral tracer distribution. This may result in different pharmacokinetic profiles in different tumor entities. In a small series of patients with different tumors, different kinetics from 1 h to 3 hrs p.i. was seen (*32*). If this observation is confirmed in a larger number of patients, this may have an impact on the indication of a FAPI-based endoradiotherapy: tumors with a longer retention may respond better than tumors with a fast elimination of the radiopharmaceutical. Furthermore, since different proteomes can be expected due to the different cellular origin of CAFs with variations in the expression of different CAF markers such as FAP,

αSMA or PDGFRβ are, this may result in a heterogeneous tracer uptake or other FAP targeting cells or molecules.

CONCLUSION

FAPIs are promising tracers for diagnostic applications for tumors showing a desmoplastic reaction, as well as for non-malignant diseases associated with tissue remodeling such as myocardial infarction, sarcoidosis, chronic inflammation, fibrosis of lung, liver and kidney, rheumatoid arthritis and possibly also artherosclerosis.

For FAPI-based endoradiotherapy the physical half-life of the radionuclide has to be adjusted to the retention time: radionuclides with shorter half-lives seem to be preferable than radionuclides with a longer half-life. This would favor the use of ^{188}Re, ^{153}Sm, ^{213}Bi or ^{212}Pb. Since CAFs are involved in many tumor supporting processes such as angiogenesis, chemoresistance and resistance to immunotherapy, combination therapies of FAP-targeted endoradiotherapy with radiation therapy, chemotherapy and immunotherapy may lead to a synergizing effect and represent an exciting future research area.

DISCLOSURE STATEMENT

Patent application (EP 18155420.5) for quinoline based FAP targeting agents for imaging and therapy in nuclear medicine (UH). Jens Siveke reports research funding from Celgene and BMS, personal fees from AstraZeneca, BMS, Celgene, Immunocore, Novartis and Roche, holds ownership in FAPI Holding (<3%). Uwe Haberkorn holds ownership in FAPI Holding (<3%).

REFERENCES

1. Zi F, He J, He D, et al. Fibroblast activation protein α in tumor microenvironment: recent progression and implications. *Mol Med Rep*. 2015; 11:3203-3211.

2. Bussard KM, Mutkus L, Stumpf K, et al. Tumor-associated stromal cells as key contributors to the tumor microenvironment. *Breast Cancer Res*. 2016;18:84 doi: 10.1186/s13058-016-0740-2

3. Henry LR, Lee HO, Lee JS, et.al. Clinical implications of fibroblast activation protein in patients with colon cancer. *Clin Cancer Res*. 13: 1736-1741, 2007.

4. Cohen SJ, Alpaugh RK, Palazzo I, et al. Fibroblast activation protein and its relationship to clinical outcome in pancreatic adenocarcinoma. *Pancreas*. 2008;37:154-158.

5. Gascard P, Tlsty TD. Carcinoma-associated fibroblasts: orchestrating the composition of malignancy. *Genes Dev*. 2016;30:1002-1019.

6. Bu L, Baba H, Yoshida N, et al. Biological heterogeneity and versatility of cancer-associated fibroblasts in the tumor microenvironment. *Oncogene*. 2019;38:4887-4901.

7. Scanlan MJ, Raj BK, Calvo B, et al. Molecular cloning of fibroblast activation protein alpha, a member of the serine protease family selectively expressed in stromal fibroblasts of epithelial cancers. *PNAS*. 1994;91:5657-5661.

8. Liu F, Qi L, Liu B, et al. Fibroblast activation protein overexpression and clinical implications in solid tumors: a meta-analysis. *PLoS One*. 2015, 10, e0116683

9. Busek P, Mateu R, Zubal M, et al. Targeting fibroblast activation protein in cancer – prospects and caveats. *Front Bioscience*. 2018;23:1933-1968.

10. Puré E, Blomberg R. Pro-tumorigenic roles of fibroblast activation protein in cancer: back to the basics. *Oncogene*. 2018;37:4343-4357.

11. Hamson EJ, Keane FM, Tholen S, et al. Understanding fibroblast activation protein (FAP): substrates, actiivities, expression and targeting for cancer therapy. *Proteomics Clin Apll*. 2014;8:454-63.

12. Goldstein LA, Ghersi G, Pineiro-Sanchez ML, et al. Molecular cloning of seprase: a serine integral membrane protease from human melanoma. *Biochim Biophys Acta*. 1997;1361:11-19 ss DOI:10.1016/S0925-5539(97)00032-X

13. Ghersi G, Zhao Q, Salamone M, et al. The protease complex consisting of dipeptidyl peptidase IV and seprase plays a role in the migration and invasion of human endothelial cells in collagenous matrices. *Cancer Res*. 2006;66:4652-4661.

14. Egger C, Cannet C, Gerard C, et al. Effects of the fibroblast activation protein inhibitor, PT100, in a murine model of pulmonary fibrosis. *Eur J Pharmacol*. 2017;809:64-72.

15. Uitte de Willige S, Malfliet JJ, Janssen HL, et al. Increased N-terminal cleavage of alpha-2-antiplasmin in patients with liver cirrhosis. *J Thromb Haemost*. 2013;11:2029-2036.

16. Tillmanns J, Hoffmann D, Habbaba Y, et al. Fibroblast activation protein alpha expression identifies activated fibroblasts after myocardial infarction. *J Mol Cell Cardiol*. 2015;87:194-203.

17. Nagaraju CK, Dries E, Popovic N, et al. Global fibroblast activation throughout the left ventricle but localized fibrosis after myocardial infarction. *Sci Rep*. 2017;7:10801.

18. Jacob M, Chang L, Pure E. Fibroblast activation protein in remodeling tissues. *Curr Mol Med*. 2012;12:1220-1243.

19. Narra K, Mullins SR, Lee HO, et al. Phase II trial of single agent ValboroPro (Talabostat) inhibiting fibroblast activation protein in patients with metastatic colorectal cancer. *Cancer Biol Ther*. 2007;6: 1691-1699. DOI: 10.4161/cbt.6.11.4874

20. Eager RM, Cunningham CC, Senzer NN, et al. Phase II trial of talabostat and docetaxel in advanced non-small cell lung cancer. *Clin Oncology*. 2009;421;464-472.

21. Eager RM, Cunningham CC, Senzer NN, et al. Phase II assessment of talabostat and cisplatin in second-line stage IV melanoma. *BMC Cancer*. 2009;9:263 DOI: 10.1186/1471-2407-9-263

22. Jansen K, Heirbaut L, Cheng JD, et al. Selective inhibitors of fibroblast activation protein (FAP) with a (4-Quinolinoyl)-glycyl-2-cyanopyrrolidine scaffold. *ACS Med Chem Lett*. 2013;4:491-496.

23. Jansen K, Heirbaut L, Verkerk R, et al. Extended structure–activity relationship and pharmacokinetic investigation of (4-Quinolinoyl)glycyl-2-cyanopyrrolidine inhibitors of fibroblast activation protein (FAP). *J Med Chemistry*. 2014;57:3053-3074.

24. Brennen WN, Isaacs JT, Denmeade SR. Rationale behind targeting fibroblast activation protein-expressing carcinoma-associated fibroblasts as a novel chemotherapeutic strategy. *Mol Cancer Ther*. 2012;11:257-266.

25. Ke M-R, Chen S-F, Peng X-H, et al. A tumor-targeted activatable phthalocyanine-tetrapeptide-doxorubicin conjugate for synergistic chemo-photodynsmic therapy. *Eur J Med Chemistry*. 2017;127:200-209.

26. Sounni E, Noel A. Targeting the tumor microenvironment for cancer therapy. *Clin Chemistry*. 2013;59:85-93.

27. Ostermann E, Garin-Chesa P, Heider KH, et al. Effective immunoconjugate therapy in cancer models targeting a serine protease of tumor fibroblasts. *Clin Cancer Res*. 2008;14:4584-4592. DOI: 10.1158/1078-0432.CCR-07-5211.

28. Lo A, Wang L-CS, Scholler J, et al. Tumor-promoting desoplasia is disrupted by depleting FAP-expressing stromal cells. *Cancer Res*. 2015,74:2800-2810.

29. Loeffler M, Krüger JA, Niethammer AG, et al. Targeting tumor-associated fibroblasts improves cancer chemotherapy by increasing intratumoral drug uptake. *J Clin Inverst*. 2006;116:1955-1962

30. Zimmermann C BJ, Joyal J, Marquis J, et al. Selective seprase inhibitors. Patent US 2010/0098633 A1. 2010.

31. Loktev A, Lindner T, Mier W et al. A new method for tumor imaging by targeting cancer associated fibroblasts. *J Nucl Med*. 2018;59:1423-1429.

32. Loktev A, Lindner T, Burger EM, et al. Development of novel FAP-targeted radiotracers with improved tumor retention. *J Nucl Med*. 2019;60:1421-1429.

33. Lindner T, Loktev A, Altmann A et al. Development of quinoline based theranostic ligands for the targeting of fibroblast activation protein. *J Nucl Med*. 2018;59:1415-1422.

34. Giesel F, Kratochwil C, Lindner T et al. FAPI-PET/CT: biodistribution and preliminary dosimetry estimate of two DOTA-containing FAP-targeting agents in patients with various cancers. *J Nucl Med*. 2019;60:386-392.

35. Kratochwil C, Flechsig P, Lindner T et al. FAPI-PET/CT: mean intensity of tracer-uptake (SUV) in 28 different kinds of cancer. *J Nucl Med.* 2019;60:801-805.

36. Meyer C, Dahlbom M, Lindner T, et al. Radiation dosimetry and biodistribution of ^{68}Ga-FAPI-46 PET imaging in cancer patients. *J Nucl Med*. 2020;61:1171-1177.

37. Moon ES, Elvas F, Vliegen G, et al. Targeting fibroblast activation protein (FAP): next generation PET radiotracers using squaramide coupled bifunctional DOTA and DATA(5m) chelators. *EJNMMI Radiopharm Chem*. 2020 Jul 29;5(1):19. doi: 10.1186/s41181-020-00102-z.

38. Toms J, Kogler J, Maschauer S, et al. Targeting fibroblast activation protein: radiosynthesis and preclinical evaluation of an ^{18}F-labeled FAP inhibitor. *J Nucl Med*. 2020 Apr 24:jnumed.120.242958. doi: 10.2967/jnumed.120.242958. Online ahead of print.

39. Giesel F, Adeberg S, Syed M, et al. FAPI-74 PET/CT using either ^{18}F-AlF or cold-kit ^{68}Ga-labeling: biodistribution, radiation dosimetry and tumor delineation in lung cancer patients. *J Nucl Med*. 2020 Jun 26:jnumed.120.245084. doi: 10.2967/jnumed.120.245084. Online ahead of print.

40. Lindner T, Altmann A, Kraemer S, et al. Design and development of ^{99m}Tc labeled FAPI-tracers for SPECT-imaging and ^{188}Re therapy. *J Nucl Med*. 2020 Mar 13:jnumed.119.239731. doi: 10.2967/jnumed.119.239731. Online ahead of print.

41. Chen H. Pang Y, Wu J, et al. Comparison of (^{68}Ga)Ga-DOTA-FAPI-04 and (^{18}F)FDG PET/CT for the diagnosis of primary and metastatic lesions in patients with various types of cancer. *Eur J Nucl Med Mol Imaging*. 2020;47:1820-1832

42. Chen H, Zhao L, Ruan D, et al. Usefulness of [^{68}Ga]Ga-DOTA-FAPI-04 PET/CT in patients presenting with inconclusive [^{18}F]FDG PET/CT findings. *Eur J Nucl Med Mol Imaging*. 2020 Jun 25. doi: 10.1007/s00259-020-04940-6. Online ahead of print.

43. Shi X, Xing H, Yang X, et al. Fibroblast imaging of hepatic carcinoma with ^{68}Ga-FAPI-04 PET/CT: a pilot study in patients with suspected hepatic nodules. *Eur J Nucl Med Mol Imaging*. 2020 May 29. doi: 10.1007/s00259-020-04882-z. Online ahead of print.

44. Röhrich M, Loktev A, Wefers AK, et al. IDH-wildtype glioblastomas and grade III/IV IDH-mutant gliomas show elevated tracer uptake in fibroblast activation protein-specific PET/CT. *Eur J Nucl Med Mol Imaging*. 2019;46:2569-2580.

45. Windisch P, Röhrich M, Regnery S, et al. Fibroblast activation protein (FAP) specific PET for advanced target volume delineation in glioblastoma. *Radiotherapy and Oncology* 150 (2020) 159–163.

46. Syed M, Flechsig P, Liermann J, et al. Fibroblast activation protein inhibitor (FAPI) PET for diagnostics and advanced targeted radiotherapy in head and neck cancers. *Eur J Nucl Med Mol Imaging*. 2020 May 23. doi: 10.1007/s00259-020-04859-y. Online ahead of print.

47. Koerber SA, Staudinger F, Kratochwil C, et al. The role of FAPI-PET/CT for patients with malignancies of the lower gastrointestinal tract - first clinical experience. *J Nucl Med*. 2020 Feb 14:jnumed.119.237016. doi: 10.2967/jnumed.119.237016. Online ahead of print.

48. Laverman P, van der Geest T,Terry SY, et al. Immuno-PET and immuno-SPECT of rheumatoid arthritis with radiolabeled anti-fibroblast activation protein antibody correlates with severity of arthritis. *J Nucl Med.* 2015;56:778-783.

49. Terry SY, Koenders MI, Franssen GM, et al. Monitoring therapy response of experimental arthritis with radiolabeled tracers targeting fibroblasts, macrophages, or integrin alphavbeta3. *J Nucl Med.* 2016;57:467-472.

50. van der Geest T, Laverman P, Gerrits D, et al. Liposomal treatment of experimental arthritis can be monitored noninvasively with a radiolabeled anti-fibroblast activation protein antibody. *J Nucl Med.* 2017;58:151-155.

51. Luo Y, Pan Q, Yang H, et al. Fibroblast activation protein targeted PET/CT with ^{68}Ga-FAPI for imaging IgG4-related disease: comparison to ^{18}F-FDG PET/CT. *J Nucl Med*. 2020 Jun 8:jnumed.120.244723. doi: 10.2967/jnumed.120.244723. Online ahead of print.

52. Schmidkonz C, Rauber S, Atzinger A, et al. Disentangling inflammatory from fibrotic disease activity by fibroblast activation protein imaging. *Ann Rheum Dis*. 2020 Jul 21:annrheumdis-2020-217408. doi: 10.1136/annrheumdis-2020-217408. Online ahead of print.

53. Varasteh Z, Mohanta S, Robu S, et al. Molecular imaging of fibroblast activity after myocardial infarction using a ^{68}Ga-Labeled fibroblast activation protein inhibitor, FAPI-04. *J Nucl Med*. 2019;60:1743-1749.

54. Totzeck M, Siebermair J, Rassaf T, et al. Cardiac fibroblast activation detected by positron emission tomography/computed tomography as a possible sign of cardiotoxicity. *Eur Heart J*. 2020;41:1060.

55. Watabe T, Liu Y, Kaneda-Nakashima K, et al. Theranostics targeting fibroblast activation protein in the tumor stroma: ^{64}Cu- and ^{225}Ac-labeled FAPI-04 in pancreatic cancer xenograft mouse models. *J Nucl Med*. 2020;61:563-569.

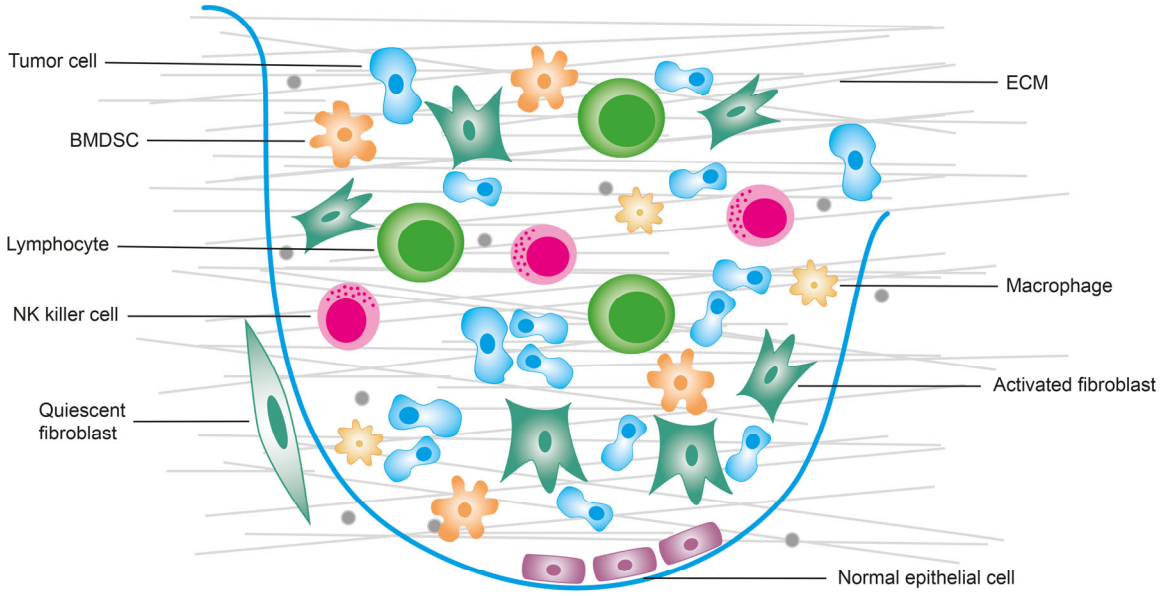

FIGURE 1: The tumor microenvironment consists of tumor cells and non-tumor cells such as bone marrow derived stem cells (BMDSC), B and T lymphocytes, NK killer cells, normal epithelial cells, activated fibroblasts (CAFs) and macrophages (T1 and T2). ECM: extracellular matrix. Modified according to: Kalluri R. The biology and function of fibroblasts in cancer. Nature Reviews Cancer 2016;16:582. https://doi.org/10.1038/nrc.2016.73

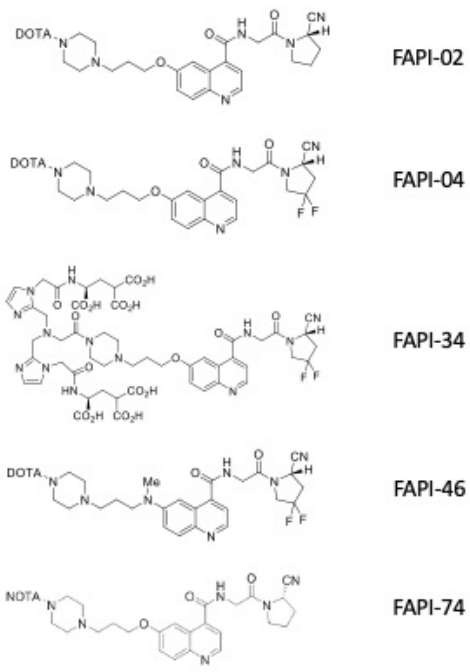

FIGURE 2: Structures of FAPI tracers used in clinical application.

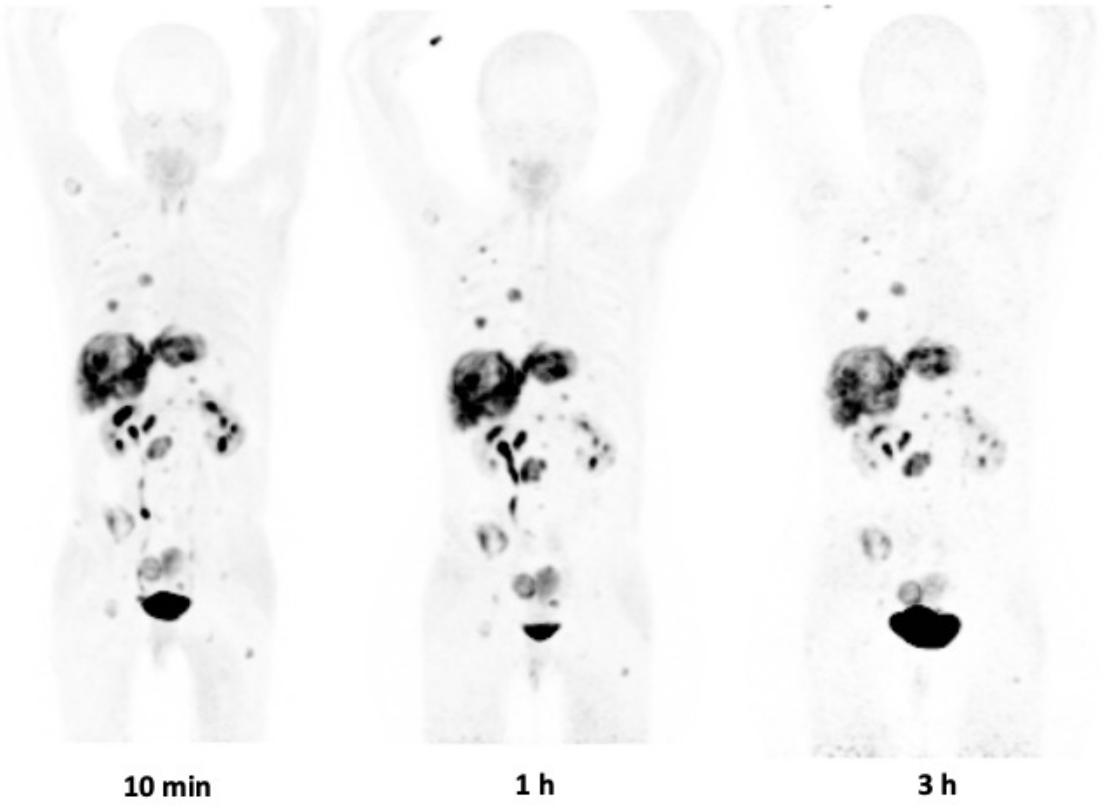

FIGURE 3: Maximum intensity Projections (MIP) at 10 min, 1 h and 3 hrs after administration of FAPI-46 in a patient with metastasized colorectal cancer. Due to a rapid tumor uptake and a very fast clearance high contrast images are possible even at 10 min p.i.

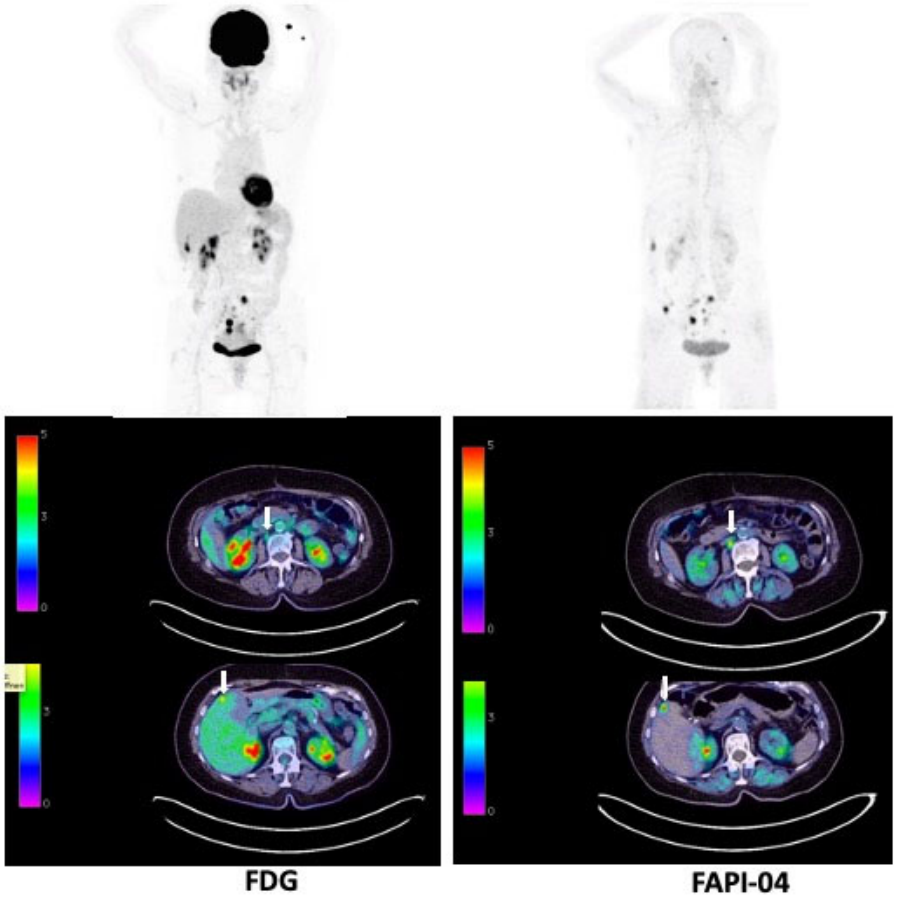

FIGURE 4: Comparison of FDG-PET/CT and FAPI-46-PET/CT in a patient with metastasized ovarian cancer. Maximum intensity Projections (MIP) and transaxial slices at 1 h p.i. The metastatic lesions in liver and lymph nodes are better seen with FAPI (white arrows).

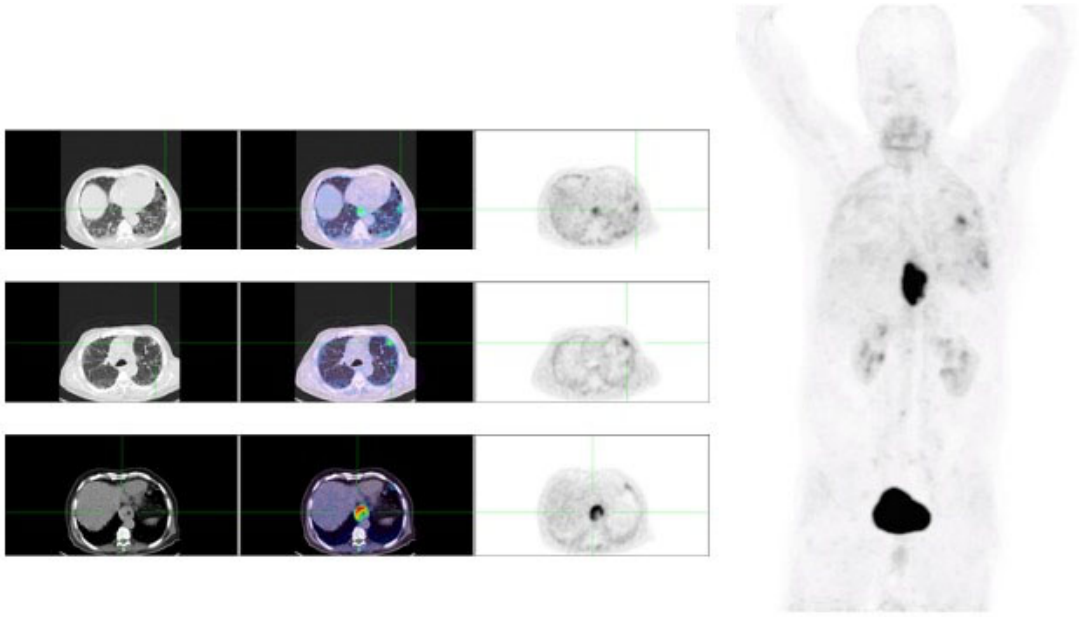

FIGURE 5: FAPI-04-PET/CT of a patient with esophageal cancer and lung fibrosis. Left: Transaxial slices (CT, fusion image and PET alone); right: maximum intensity projection (MIP).